Dalton Transactions

Accepted Manuscript

ROYAL SOCIETY OF CHEMISTRY

www.rsc.org/dalton

Pillared metal organic frameworks for luminescence sensing of small molecules and metal ions in aqueous solution

Fu-Hong Liu,[ab] Chao Qin,[*a] Yan Ding,[b] Han Wu,[a] Kui-Zhan Shao[a] and Zhong-Min Su[*a]

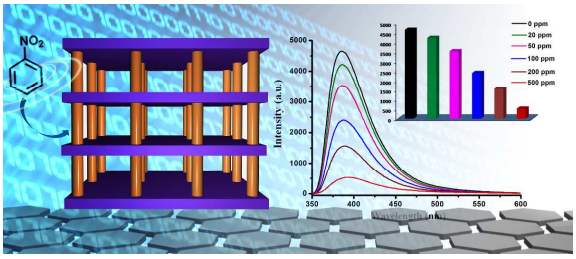

Two pillared-layer MOFs as luminescent probes with multifunctional sensitivity to detect metal ions and small molecules were reported. Our results show that the luminescence intensity of **1a** and **2a** are highly sensitive to Fe^{3+} and Cd^{2+} ions and small molecules such as acetone and nitrobenzene.

Journal Name

RSCPublishing

ARTICLE

Pillared metal organic frameworks for luminescence sensing of small molecules and metal ions in aqueous solution

Cite this: DOI: 10.1039/x0xx00000x

Received 00th January 2012,
Accepted 00th January 2012

DOI: 10.1039/x0xx00000x

www.rsc.org/

Fu-Hong Liu,[ab] Chao Qin,[*a] Yan Ding,[b] Han Wu,[a] Kui-Zhan Shao[a] and Zhong-Min Su[*a]

Two novel pillared MOFs (metal organic frameworks) $[Zn_2(trz)_2(tda)]\cdot DMA\ CH_3OH$ (**1**) and $[Zn_2(trz)_2(bpdc)]\cdot DMA$ (**2**) were obtained under solvothermal condition. The resulted MOFs show similar structures but with different interlayer distances based on different carboxylate ligands. **1** and **2** display a certain degree of framework stabilities in both acid/base solutions and water. The luminescence intensity of activated phase **1a** and **2a** are sensitive to metal ions, particularly $Fe^{3+}$and Cd^{2+} ions. Furthermore, luminescent properties of **1a** and **2a** well dispersed in different solvents have also been investigated systematically, which demonstrate distinct solvent-dependent luminescent spectra with emission intensities significantly quenched toward acetone, nitrobenzene and trinitrotoluene.

Introduction

The current increasing interest in designing metal−organic frameworks (MOFs) has been significantly provoked not only because of their aesthetically beautiful architectures but also their potential applications, such as gas storage and separation,[1-2] heterogeneous catalysis,[3] and small-molecule sensing.[4] Employing rational design strategies to construct porous materials with high surface areas, predictable structure, and tunable pore sizes is still one of the most compelling challenges to chemists. One strategy for the construction of porous MOFs is based primarily on the proper selection of inorganic building blocks as nodes, such as Zn_4O or paddle wheels, which are called secondary building units (SBUs), and rigid organic bridging ligands as linkers. Pillared-layer structure, have proved to be another efficient route to controllably construct frameworks.[5-6] Because simple modification of the pillar module can control the channel size and shape, since the length of pillar and the pore size are closely related. Moreover, the degree of flexibility (or rigidity) and physical properties such as hydrophilic/hydrophobic character, hydrogen bonding, and open metal site can be adjusted by the functionalization of the pillar ligands.[7] In addition to the presence of chemical functionalities on the pore surface, flexible MOFs can undergo several types of dynamic structural changes resulting in high selectivity for guest inclusion.[8]

A number of luminescent materials sensing small molecules or metal ions are widely exploited in many areas, such as luminescent probes in biomedical assays, fluorescent lighting and luminescent probes for chemical species.[9] In fact, the MOF chemosensors have obtained considerable attention owing to their intriguing photo-physical properties, such as evident Stokes shifts, excitation in the visible range and relatively long lifetimes.[10] Over the past few years, several lanthanide MOFs have been exploited luminescent properties to sense organic solvents, aromatics, vapors, and metal ions by Chen and Liu et al.[11] Liu reported the first lanthanide MOF $Na[EuL(H_2O)_4]_3\cdot 2H_2O$ (L = 1,4,8,11-tetraazacyclotetradecane-1,4,8,11-tetrapropionic acid) for sensing cations.[11a] Chen et al. reported Eu^{3+} sites in Eu(BTC) for sensing of small molecules.[11b] Several transition metal–organic frameworks used for molecular sensing have also been reported, for example, the sensing of nitric oxide in Cu−TCA,[12] solvent sensing in ZnL (L = 4,4′-stilbenedicarboxylic acid),[13] selective detection of nitro explosives in $[Cd(NDC)_{0.5}(PCA)]$.[14] The design and synthesis of MOF sensors aimed at the convenient detection of volatile organic solvent molecules and special metal-selective fluorescence properties have attracted tremendous interest in coordination chemistry.

In this work, we report two isostructural pillared-layer MOFs based on Zn^{2+}, 1-H-1,2,4-triazole and H_2tda (2,5-thiophenedicarboxylic acid)/H_2bpdc (4,4'-diphenyldicarboxylic acid) ligands. They display a certain degree of framework stabilities in both acid/base solutions and water. The phase purities of bulk products were confirmed using X-ray powder diffraction (XRPD) (Fig. S2). Considering metal-organic frameworks constructed from d^{10} metal ions and conjugated organic linkers are promising candidates for potential photoactive materials, luminescent properties of activated **1a** and **2a** dispersed in different metal ions and solvents have been investigated systematically.

Experimental section

General information

All chemical materials were purchased from commercial sources and used without further purification. The FT-IR spectra were recorded from KBr pellets in the range 4000–400 cm^{-1} on a Mattson Alpha-Centauri spectrometer. XRPD

patterns were recorded on a Siemens D5005 diffractometer with Cu Kα (λ = 1.5418 Å) radiation in the range of 3−60° at a rate of 5°/min. The C, H, and N elemental analyses were conducted on a Perkin-Elmer 2400CHN elemental analyzer. TG curves were performed on a Perkin–Elmer TG-7 analyzer heated from room temperature to 1000 ºC at a ramp rate of 5 °C/min under nitrogen. The photoluminescence spectra were measured on a Perkin-Elmer FLS-920 Edinburgh Fluorescence Spectrometer.

Crystal structure determination

Single-crystal X-ray diffraction data for **1** and **2** were recorded by using a Bruker Apex CCD diffractometer with graphite-monochromated Mo-Kα radiation (λ = 0.71069 Å) at 293 K. Absorption corrections were applied by using a multi-scan technique. All the structures were solved by Direct Method of SHELXS-97 and refined by full-matrix least-squares techniques using the SHELXL-97 program within WINGX. Non-hydrogen atoms were refined with anisotropic temperature parameters. The detailed crystallographic data and structure refinement parameters for **1** and **2** are summarized in Table S1.

Synthesis of $[Zn_2(trz)_2(tda)]\cdot DMA\ CH_3OH$ (1)

A mixture of $Zn(NO_3)_2\cdot 6H_2O$ (60 mg, 0.2 mmol), 1, 2, 4-triazole (14 mg, 0.2 mmol), and H_2tda (14 mg, 0.1 mmol) was dissolved in 6 mL of DMA/MeOH (1:1, v/v). The final mixture was placed in a Parr Teflon-lined stainless steel vessel (15 mL) under autogenous pressure and heated at 100 °C for 3 days. Colorless crystals were obtained, which were washed with mother liquid, and dried under ambient conditions. Anal. Calcd for $C_{15}H_{19}N_7O_6SZn_2$: C, 32.39; H, 3.44; N, 17.63. Found: C, 32.14; H, 3.18; N, 17.35. IR (KBr, cm^{-1}): 2340.78 (w), 849.36 (w), 3030.45 (w), 2936.57 (w), 3625.97 (w), 589.94 (w), 408.88 (w), 3543.32 (w), 920.96 (w), 474.88 (w), 538.25 (w), 515.30 (w), 3099.75 (m), 1262.14 (m), 1039.32 (m), 824.63 (m), 1722.20 (m), 1217.93 (m), 1171.77 (m), 1007.69 (m), 774.20 (m), 1300.69 (m), 668.73 (s), 1092.77 (s), 1373.23 (s), 1525.08 (s), 1623.38 (s).

Synthesis of $[Zn_2(trz)_2(bpdc)]\cdot DMA$ (2)

A mixture of $Zn(NO_3)_2\cdot 6H_2O$ (60 mg, 0.2 mmol), 1, 2, 4-triazole (14 mg, 0.2 mmol), and H_2bpdc (24 mg, 0.1 mmol) was dissolved in 6 mL of DMA/MeOH (1:1, v/v). The final mixture was placed in a Parr Teflon-lined stainless steel vessel (15 mL) under autogenous pressure and heated at 100 °C for 3 days. Colorless crystals were obtained, which were washed with mother liquid, and dried under ambient conditions. Anal. Calcd for $C_{22}H_{21}N_7O_5Zn_2$: C, 44.46; H, 3.56; N, 16.50. Found: C, 44.13; H, 3.23; N, 16.19. IR (KBr, cm^{-1}): 731.22 (w), 3646.96 (w), 921.28 (w), 2349.78 (w), 2486.85 (w), 1748.10 (w), 474.51 (w), 894.47 (w), 2932.34 (w), 446.88 (w), 3445.41 (w), 1217.19 (w), 856.72 (w), 474.51 (w), 3126.72 (w), 1436.48 (w), 774.15 (w), 1090.77 (m), 1078.4 (m), 1275.95 (m), 1498.02 (m), 1398.07 (m), 1313.27 (s), 1164.47 (s), 1008.03 (s), 1510.96 (s), 1623.87 (s), 664.32 (s).

Activation of 1a and 2a

The samples **1** and **2** were immersed in CH_2Cl_2 for 24 h, and the extracts were decanted. Fresh CH_2Cl_2 was subsequently added, and the crystals were allowed to stay for an additional 24 h to remove the nonvolatile dimethylacetamide (DMA). After the removal of dichloromethane by decanting, the activated samples **1a** and **2a** were obtained by drying under a dynamic vacuum at 80 ºC overnight.

The metal ions sensing experiment

1a and **2a** powder (50 mg) into aqueous solution (10 mL) of $M(NO_3)x$ (M = Cd^{2+}, Fe^{3+}, Co^{2+}, Zn^{2+}, Pb^{2+}, or Cu^{2+}). Then, the M-incorporated **1a** and **2a** were isolated by filtration and drying at room temperature for 24 h before fluorescence measurements.

The solvent sensing experiment

The solvent sensing experiment has been performed as follows: finely ground samples of **1a** and **2a** (3 mg) was immersed in different organic solvents (3 mL), treated by ultrasonication for 30 minutes, and then aged to form stable emulsions before fluorescence was measured.

Results and discussion

Crystal structure description

Solvothermal reactions of $Zn(NO_3)_2$, 1,2,4-triazole, and H_2tda or H_2bpdc in DMA/MeOH solvent at 100 ° C for 3 days yielded two crystalline products, **1** and **2**, respectively. The crystallographic parameters of two compounds are given in Supporting Information Table S1. **1** and **2** are all pillared-layer structures based on the Zn-triazolate layers and dicarboxylate pillars. Single-crystal structure analysis reveals that **1** crystallizes in the tetragonal system, space group *I*/4*m*. As shown in Fig 1, the asymmetric unit of **1** contains one Zn atom, one-half H_2tda ligand and one 1, 2, 4-triazole ligand. Each Zn^{2+} ion is five-coordinated with two O atoms from one carboxyl group of one individual H_2tda ligand, and three N atoms from three individual 1,2,4-triazole (Zn-N 2.025-2.010 Å, Zn-O 1.995-2.473 Å). Each triazole ligand binds to three Zn atoms through 1,2,4-position N atoms, and each H_2tda ligand links two Zn^{2+} ions through its two carboxylate ends. Moreover, the triazole ligands link the Zn^{2+} to form a two-dimensional (2D) layer. The adjacent {Zn(trz)} layers are further connected by the H_2tda pillars and extended into a 3D pillared-layer structure. The spaces between the layers are occupied by DMA and CH_3OH molecules. The solvent accessible volumes of 40.7 % (1968.1 $Å^3$) per unit cell (4836.9 $Å^3$), is calculated by PLATON.[15] For the channels along the *b* axis, the dimension of channels of **1** and **2** have the sizes of 10.1×6.5 $Å^2$ and 15.1×6.5 $Å^2$ ($a \times c$), with the tda ligands replaced by the longer carboxylate ligands bpdc. And the channels along the c axis, **1** and **2** both have the dimension of 6.5 × 6.5 $Å^2$ ($a \times b$) because of the same two-dimensional (2D) layer. Topologically, both frameworks of **1** and **2** present the same 6-connected **pcu** network, when considering

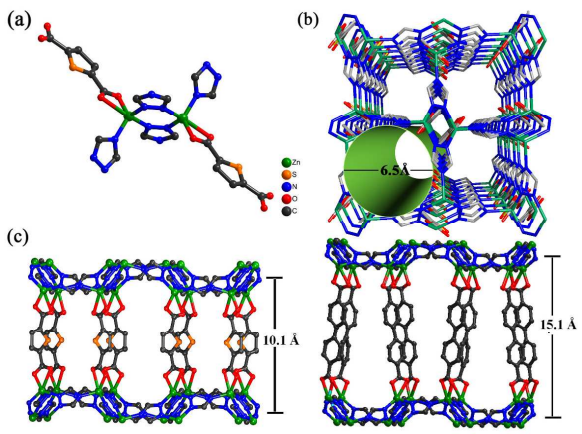

Fig. 1 (a) The coordination environment of the Zn(II) center in **1**. The hydrogen atoms are omitted for clarity (Zn, green; S, yellow; N, blue; O, red; C, gray). (b) The view of **1** along the *c* axis. (c) Representations of pillared-layer structures of **1** (left) and **2** (right).

the {Zn(trz)} unit as the 6-connected node and the dicarboxylate as the linker.

Thermal and Chemical stabilities

The purities of the as-synthesized **1** and **2** were confirmed by X-ray powder diffraction (XRPD) patterns. (Fig. S2). The TGA curve of **1** shows obvious weight loss of 20.1 % in the temperature range 56-275 °C, corresponding to the loss of one CH_3OH and one DMA molecules (calcd 21.5 %). And the TG curve of **2** shows the first weight loss of one DMA molecule in the range 56-224 °C (calcd 14.7%). The TG curves of **1** and **2** indicate that can be thermally stable around 315 °C and 375 °C (Fig 2).

Thermogravimetry analyses showed that **1** and **2** have high thermal stability. Stability is essential for the technological use of MOFs, thus, we examined the stabilities of **1** and **2** for future practical applications. To investigate the water stabilities, compounds **1** and **2** were tested in water at ambient temperature and 100 °C. Fig 3 show that the framework of **1** and **2** remain unchanged after exposure to water 24 h. The XRPD patterns exhibit similar shape and intensity When **1** and **2** were immersed in hydrochloric acid solution (pH = 2) or sodium

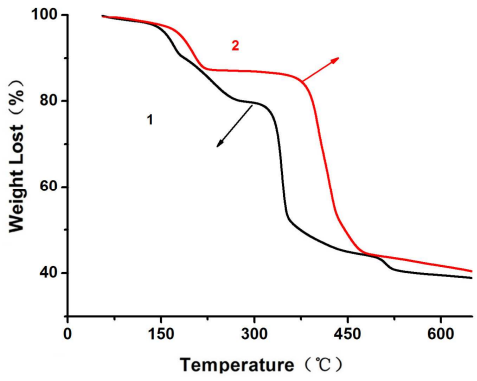

Fig. 2 TGA curves for **1** (black) and **2** (red).

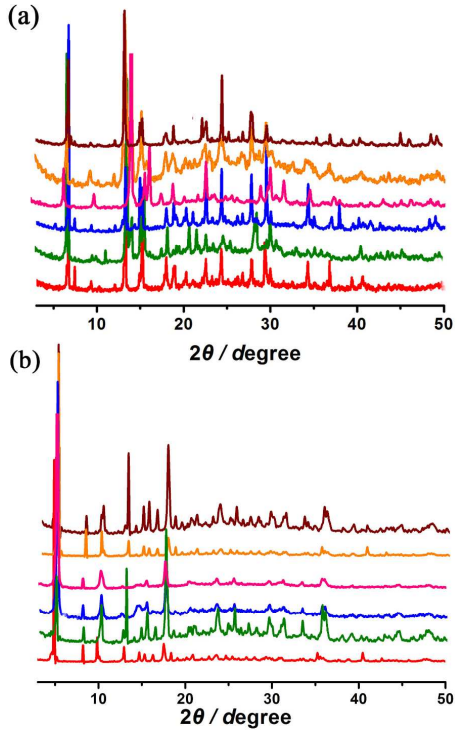

Fig. 3 XRPD patterns of **1** (a) and **2** (b): as-synthesized (red), treated in ambient temperature (green), boiling water (blue), after soaking in acid (pH = 2, pink), alkaline solutions (pH = 12, yellow) and exposed in air for 3 months (wine).

hydroxide solution (pH = 12) for 24 h. Even exposed to air for 3 months, no significant change of the XRPD patterns were found for the samples (Fig. 3).

Luminescence behaviors and sensing properties

Metal-organic frameworks constructed from d^{10} metal ions and conjugated organic linkers are promising candidates for potential photoactive materials. Considering **1** and **2** are closely related structures with high conjugated frameworks, which allow comparative investigation of luminescence properties relative to structural features. The solid photoluminescence (PL) spectra of ligand H_2tda, H_2bpdc, the activated phases **1a** and **2a** were recorded at room temperature (Fig. S6, S7). To examine the potential of **1a** and **2a** for the sensing of metal ions, the activated samples **1a** and **2a** were immersed in aqueous solutions containing $M(NO_3)X$ (M = Cd^{2+}, Fe^{3+}, Co^{2+}, Zn^{2+}, Pb^{2+}, or Cu^{2+}). As shown in Fig. 4, the PL intensity of **1a** and **2a** are dependent on the metal ion–aqueous solutions, particularly in the cases of $Cd(NO_3)_2$, $Zn(NO_3)_2$ and $Fe(NO_3)_3$ solutions. The Zn^{2+} and Cd^{2+} ions have enhanced sensing effect, and Fe^{3+} have quenching effect, whereas adding other metal ions, such as 1mM aqueous solutions containing Co^{2+}, Cu^{2+} had no evident effect on the emission intensity.

Cd^{2+} was selected for further enhanced luminescence studies. **1a** and **2a** were immersed in Cd^{2+}-aqueous solutions containing different concentrations of $Cd(NO_3)_2$ (Fig. S9, S10). The emission intensity of Cd-incorporated **1a** from a 100 mM aqueous solutions containing $Cd(NO_3)_2$ increased than metal-ion free **1a**, indicating the potential of **1a** for the sensing of Cd^{2+}. On the contrary, the

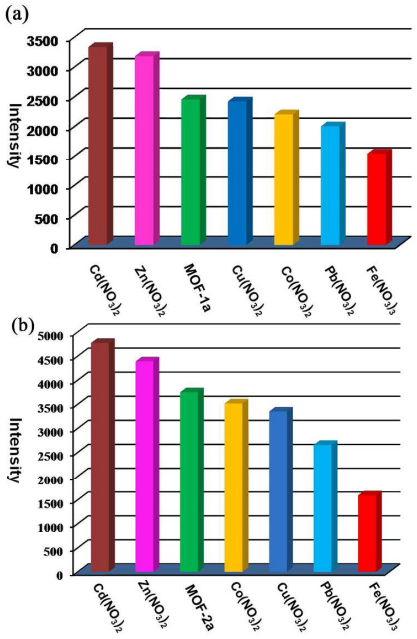

Fig. 4 Comparisons of the luminescence intensity of **1a** (a) and **2a** (b) incorporating different metal ions in 10 mM aqueous solutions of $M(NO_3)_x$ (**1a** excited and monitored at 313 nm and 391 nm; **2a** excited and monitored at 326 nm and 388 nm respectively).

luminescence intensity decreases proportionally to the concentration of Fe^{3+} (Fig. S9, S10). The interesting quenching effect of Fe^{3+} and the enhancing effect of Cd^{2+} to **1a** and **2**a provide a perspective for further sensing material studies. The intrusion of various metal ions into the 3D compounds did not distort or bring major change to the structures. The PXRD patterns of **1a** and **2a** incorporated with different metal-ions are identical to as-synthesized (Fig. 5), which suggests that the crystal lattices remain robust after the treatment. PXRD patterns further confirm the high framework stability of **1** and **2**.

Meanwhile, the luminescence properties of **1a** and **2a** in different solvent emulsions were investigated. The solvents used are dichloromethane (CH_2Cl_2), acetonitrile, ethanol, methanol, *n*-hexane, ethyl acetate, N, N-dimethylformamide (DMF), N, N-dimethylacetamide (DMA), acetone, benzene, and nitrobenzene. The most interesting feature is that its PL spectrum is largely dependent on the solvent molecules, particularly in the case of CH_2Cl_2, acetone and nitrobenzene, which exhibit the most significant enhancing and quenching effects, respectively (Fig. 6). Such solvent-dependent luminescence properties are of interest for the sensing of acetone and nitrobenzene solvent molecules.

When the acetone solvent content was gradually added and increased to **1a**-MeOH and **2a**-MeOH standard emulsion, the fluorescence intensity of the standard emulsion gradually decreased with the addition of acetone solvent (Fig. 7). The fluorescence decrease was nearly proportional to the acetone concentration and the system ultimately reaches the equilibrium state. The efficient quenching of acetone in this system can be ascribed to the physical interaction of the solute and solvent, which induces the electron transfer from the excited **1a** or **2a** to electron-deficient acetone.[16] The encouraging

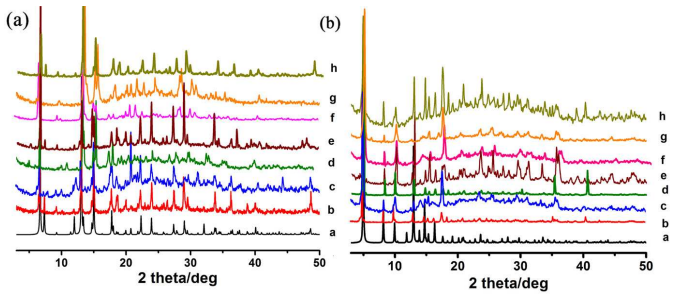

Fig. 5 Powder X-ray diffraction patterns of a) simulated from the X-ray single structure, b) activated, and diffraction patterns obtained after the introduction of various metal ions: c) Cu^{2+}, d) Zn^{2+}, e) Fe^{3+}, f) Co^{2+}, g) Cd^{2+} and h) Pb^{2+} of **1a** (a) and **2a** (b).

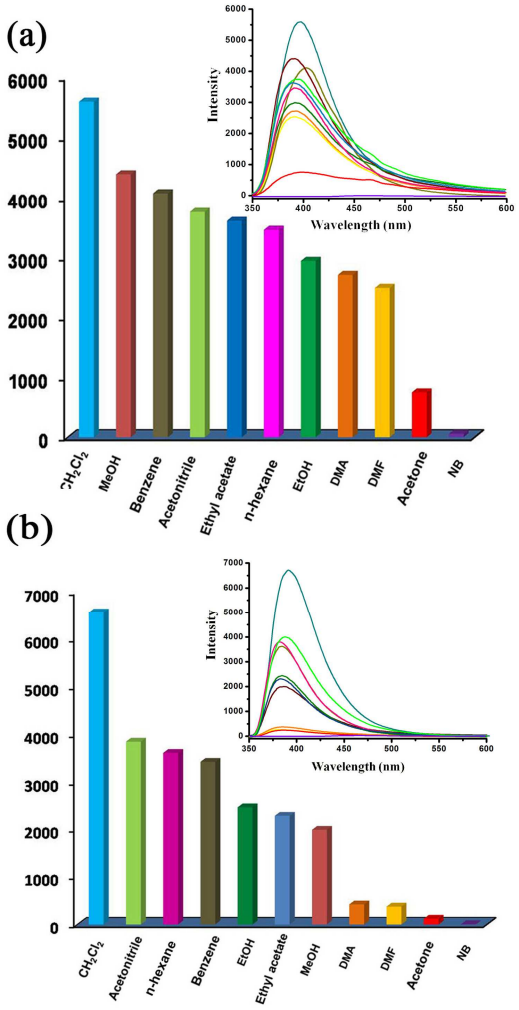

Fig. 6 Comparisons of the luminescence intensity of **1a**-solvent and **2a**-solvent emulsions at room temperature (excited at 313 nm and 310 nm, respectively) (solvent = CH_2Cl_2, acetonitrile, EtOH, *n*-hexane, ethyl acetate, benzene, MeOH, DMA, DMF, acetone and nitrobenzene).

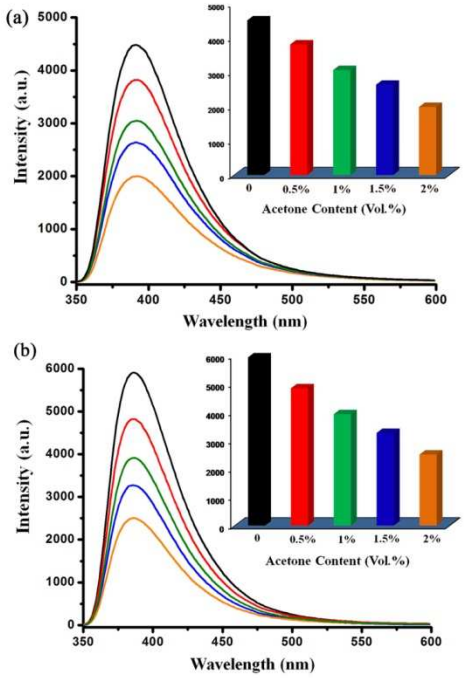

Fig. 7 Emission spectra of the dispersed (a) **1a** and (b) **2a** in CH_3OH in the presence of various contents of acetone solvent (excited at 313 nm and 310 nm, respectively).

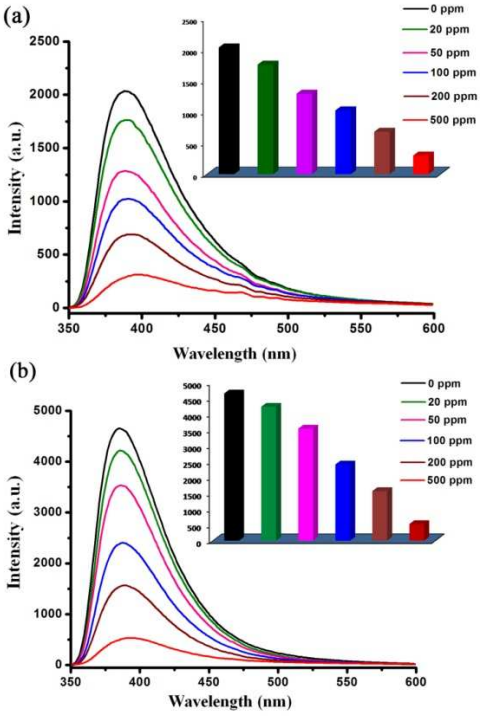

Fig. 8 Emission spectra of (a) **1a** and (b) **2a** at different nitrobenzene concentrations in CH_3OH (excited at 313 nm and 310 nm, respectively).

results reveal that **1a** and **2a** could be promising luminescent probes for detecting small molecules-acetone. Moreover, the emission intensities of the emission peaks are largely dependent on the solvent molecules, especially towards nitrobenzene, which shows a significant quenching effect. Such solvent-dependent quenching behavior is of interest for the sensing of nitrobenzene molecules, and thus it was examined in detail. A batch of emulsions of **1a** and **2a** in CH_3OH with gradually increased nitrobenzene concentration was prepared to monitor the emissive response. As seen in Fig. 8, the luminescent intensity of the emulsions significantly decreased with increasing addition of nitrobenzene. The intensity of **1a**-MeOH and **2a**-MeOH standard emulsion decreased to 50 % at only 100 ppm, 11 % at 500 ppm, which allowed us to detect small amounts of nitrobenzene in solution. The further research was carried on by soaking the crystals **1a** and **2a** at different TNT (trinitrotoluene) concentrations in CH_3OH. The results show the luminescent intensity of the emulsions decreased with gradually increased TNT concentration. The possibility of quenching mechanism is assumed to originate from the electron-withdrawing property of the nitro groups in the analytes, which results in a significant donor–acceptor electron transfer from the ligands to the electron-donating MOF structures.[17]

Conclusions

In summary, two pillared-layer MOFs as luminescent probes with multifunctional sensitivity to detect metal ions and small molecules were reported. They also display a certain degree of framework stabilities in both acid/base solutions and water. Our results show that the luminescence intensity of **1a** and **2a** are highly sensitive to Fe^{3+} and Cd^{2+} ions and small molecules such as acetone and nitrobenzene. It is expected that by further using chemically and thermally stable MOFs, such host–guest strategy may lead to some highly sensitive sensor with multifunction applications.

Acknowledgements

This work was financially supported by the NSFC of China (No. 21471027, 21171033, 21131001, 21222105), National Key Basic Research Program of China (No. 2013CB834802), The Foundation for Author of National Excellent Doctoral Dissertation of P.R.China (FANEDD) (No. 201022), Changbai mountain scholars of Jilin Province and FangWu distinguished young scholar of NENU.

Notes and references

[a]*Institute of Functional Material Chemistry, Key Laboratory of Polyoxometalate Science of Ministry of Education, Northeast Normal University, Changchun, 130024 Jilin, People's Republic of China. E-mail: qinc703@nenu.edu.cn; zmsu@nenu.edu.cn Fax: +86 431-85684009; Tel: +86 431-85099108*
[b]*Foundation Department, Jilin Business and Technology College, Changchun, 130507 Jilin, People's Republic of China.*
Electronic Supplementary Information (ESI) available: Experimental details, XRPD, TG, IR, solid photoluminescence (PL) spectra and additional figures for **1** and **2**. CCDC 1025511-1025512 (**1-2**) . For ESI and crystallographic data in CIF or other electronic format see DOI: 10.1039/x0xx00000x

1 (a) L. J. Murray, M. Dincă and J. R. Long, *Chem. Soc. Rev.*, 2009, **38**, 1294; (b) M. P. Suh, H. J. Park, T. K. Prasad and D. W. Lim, *Chem. Rev.*, 2012, **112**, 782; (c) Q. P. Lin, T. Wu, S. T. Zheng, X. H. Bu and P. Y. Feng, *J. Am. Chem. Soc.*, 2012, **134**, 784; (d) Y. Yan, I. Telepeni, S. Yang, W. Kockelmann, A. Dailly, A. J. Blake, W. Lewis, G. S. Walker, D. R. Allan, S. A. Barnett, N. R. Champness and M. Schroder, *J. Am. Chem. Soc.*, 2012, **132**, 4092; (e) J. R. Li, R. J. Kuppler and H. C. Zhou, *Chem. Soc. Rev.*, 2009, **38**, 1477.

2 (a) K. Sumida, D. L. Rogow, J. A. Mason, T. M. McDonald, E. D. Bloch, Z. R. Herm, T. H. Bae and J. R. Long, *Chem. Rev.*, 2012, **112**, 724; (b) J. R. Li, R. J. Kuppler and H. C. Zhou, *Chem. Soc. Rev.*, 2009, **38**,1477; (c) K. Sumida, D. L. Rogow, J. A. Mason, T. M. McDonald, E. D. Bloch, Z. R. Herm, T. H. Bae and J. R. Long, *Chem. Rev.*, 2012, **112** , 724.

3 (a) L. Ma, C. Abney and W. Lin, *Chem. Soc. Rev.*, 2009, **38**, 1248; (b) A. Corma, H. Garcíaand and F. X. Llabrés i Xamena, *Chem. Rev.*, 2010, **110**, 4606; (c) M. Yoon, R. Srirambalaji and K. Kim, *Chem. Rev.*, 2012, **112**, 1196; (d) J. Y. Lee, O. K. Farha, J. Roberts, K. A. Scheidt, S. T. Nguyen and J. T. Hupp, *Chem. Soc. Rev.*, 2009, **38**, 1450; (e) D. Farrusseng, S. Aguado and C. Pinel, *Angew. Chem., Int. Ed.*, 2009, **48**, 7502.

4 (a) J. H. Cui, Z. Z. Lu, Y. Z. Li, Z. J. Guo and H. G. Zheng, *Chem. Commun.*, 2012, **48**, 7967; (b) Z. Z. Lu, R. Zhang, Y. Z. Li, Z. J. Guo and H. G. Zheng, *J. Am. Chem. Soc.*, 2011, **133**, 4172; (c) Y. Li, S. S. Zhang and D. T. Song, *Angew. Chem., Int. Ed.*, 2013, **52**, 710; (d) D. X. Ma, B. Y. Li, X. J. Zhou, Q. Zhou, K. Liu, G. Zeng, G. H. Li, Z. Shi and S. H. Feng, *Chem. Commun.*, 2013, **49**, 8964.

5 (a) T. J. Prior, D. Bradshaw, S. J. Teat and M. J. Rosseinsky, *Chem. Commun.*, 2003, 500; (b) J. L. Song, H. H. Zhao, J. G. Mao and K. R. Dunbar, *Chem. Mater.*, 2004, **16**, 1884.

6 (a) M. Kondo, T. Okubo, A. Asami, S. Noro, T. Yoshitomi, S. Kitagawa, T. Ishii, H. Matsuzaka and K. Seki, *Angew. Chem., Int. Ed.*, 1999, **38**, 140; (b) Y. Diskin-Posner, S. Dahal and I. Goldberg, *Angew. Chem., Int. Ed.*, 2000, **112**, 1344; (c) D. R. Xiao, E. B. Wang, H. Y. An, Y. G. Li, Z. M. Su and C. Y. Sun, *Chem. Eur. J.*, 2006, **12**, 6528; (d) H. L. Ngo and W. Lin, *J. Am. Chem. Soc.*, 2002, **124**, 14298; (e) M. J. Zaworotko, *Chem. Commun.*, 2001, **40**, 2111.

7 (a) M. E. Kosal, J. H. Chou, S. R. Wilson and K. S.Suslick, Nat. Mater., 2002, **1**, 118; X. F. Wang, Y. B. Zhang and W. Xue, *Cryst. Growth Des.*, 2012, **12**, 1626; (c) C. Zhang, Y. Cao, J. Zhang, S. Meng, T. Matsumoto, Y. Song, J. Ma, Z. Chen, K. Tatsumi and M. G. Humphrey, *Adv. Mater.*, 2008, **20**, 1870; (d) Z. Q. Wang and S. M. Cohen *J. Am. Chem. Soc.*, 2007 , **129**, 12368; (e) S. Horike, S. Bureekaew and S. Kitagawa, *Chem. Commun.*, 2008, 471; (f) B. Liu, M. Ma, D. Zacher, A. Bétard, K. Yusenko, N. Metzler-Nolte, C. Wöll and R. A. Fischer, *J. Am. Chem. Soc.*, 2011, **133**, 1734.

8 (a) R. Matsuda, R. Kitaura, S. Kitagawa, Y. Kubota, R. V. Belosludov, T. C. Kobayashi, H. Sakamoto, T. Chiba, M. Takata, Y. Kawazoe and Y. Mita, *Nature*, 2005, **436**, 238; (b) S. Shimomura, S. Horike, R. Matsuda and S. Kitagawa, *J. Am. Chem. Soc.*, 2007, **129**, 10990; (c) S. Bourrelly, P. L. Llewellyn, C. Serre, F. Millange, T. Loiseau and G. Férey, *J. Am. Chem. Soc.*, 2005, **127**, 13519; (d) R. Matsuda, R. Kitaura, S. Kitagawa, Y. Kubota, T. C. Kobayashi, S. Horike and M. Takata, *J. Am. Chem. Soc.*, 2004, **126**, 14063;

9 (a) M. D. Allendorf, C. A. Bauer, R. K. Bhakta and R. J. T. Houk, *Chem. Soc. Rev.*, 2009, **38**, 1330; (b) L. E. Kreno, K. Leong, O. K. Farha, M. Allendorf, R. P. Van Duyne and J. T. Hupp, *Chem. Rev.*, 2012, **112**, 1105; (c) A. G. Davies, A. D. Burnett, W. Fan, E. H. Linfield and J. E. Cunningham, *Mater. Today.*, 2008, **11**, 18.

10 (a) W. Liu, T. Jiao, Y. Li, Q. Liu, M. Tan, H. Wang and L. Wang, *J. Am. Chem. Soc.*, 2004, **126**, 2280; (b) B. Gole, A. K. Bar and P. S. Mukherjee, *Chem. Commun.*, 2011, **47**, 12137; (c) N. Wei, Y. R. Zhang and Z. Bo. Han, *CrystEngComm.*, 2013, **15**, 8883.

11 (a) W. S. Liu, T. Q. Jiao, Y. Z. Li, Q. Z. Liu, M. Y. Tan, H. Wang and L. F. Wang, *J. Am. Chem. Soc.*, 2004, **126**, 2280; (b) B. Chen, Y. Yang , F. Zapata, G. N. Lin , G. Qian and E. B. Lobkovsky, *Adv. Mater.*, 2007, **19**, 1693; (c) B. Chen, L. Wang, F. Zapata, G. Qian and E. B. Lobkovsky, *J. Am. Chem. Soc.*, 2008, **130**, 6718; (d) B. Chen, L. Wang, Y. Xiao, F. R. Fronczek, M. Xue, Y. Cui and G. Qian, *Angew. Chem., Int. Ed.*, 2009, **48**, 500.

12 P. Y. Wu, J. Wang, C. He, X. L. Zhang, Y. T. Wang, T. Liu and C. Y. Duan, *Adv. Funct. Mater.*, 2012, **22**, 1698.

13 C. A. Bauer, T. V. Timofeeva, T. B. Settersten, B. D. Patterson,V. H. Liu, B. A. Simmons and M. D. Allendorf, *J. Am. Chem. Soc.*, 2007, **129**, 7136.

14 S. S. Nagarkar, B. Joarder, A. K. Chaudhari, S. Mukherjee and S. K. Ghosh, *Angew. Chem., Int. Ed.*, 2013, **52**, 2881.

15 A. L. Spek, PLATON, *A multipurpose crystallographic tool* Utrecht. University, The Netherlands, 2003.

16 (a) Z. M. Hao, X. Z. Song, M. Zhu, X. Meng, S. N Zhao, S. Q Su, W. T. Yang, S. Y. Song and H. J. Zhang, *J. Mater. Chem. A.*, 2013, **1**, 11043; (b) Y. Q. Xiao, L. B. Wang, Y. J. Cui, B. L. Chen, F. Zapata and G. D. Qian, *J. Alloys Compd.*, 2009, **484**, 601.

17 (a) H. Wang, W. T. Yang and Z. M. Sun, *Chem. Asian J.*, 2013, **8**, 982; (b) M. Guo and Z. M. Sun, *J. Mater. Chem*., 2012, **22**, 15939.

